HHS Public Access

Author manuscript

Clin Cancer Res. Author manuscript; available in PMC 2021 December 15.

Published in final edited form as:

Clin Cancer Res. 2021 June 15; 27(12): 3339–3350. doi:10.1158/1078-0432.CCR-20-4575.

Phase 1 trial of N-803, an IL-15 receptor agonist, with rituximab in patients with indolent non-Hodgkin lymphoma

Jennifer A. Foltz[1], **Brian T. Hess**[2], **Veronika Bachanova**[3], **Nancy L. Bartlett**[1], **Melissa M. Berrien-Elliott**[1], **Ethan McClain**[1], **Michelle Becker-Hapak**[1], **Mark Foster**[1], **Timothy Schappe**[1], **Brad Kahl**[1], **Neha Mehta-Shah**[1], **Amanda F. Cashen**[1], **Nancy D. Marin**[1], **Kristen McDaniels**[1], **Chaz Moreno**[1], **Matthew Mosior**[1], **Feng Gao**[1], **Obi L. Griffith**[1], **Malachi Griffith**[1], **Julia A. Wagner**[1], **Narendranath Epperla**[4], **Amy D. Rock**[5], **John Lee**[5], **Allegra A. Petti**[1], **Patrick Soon-Shiong**[5], **Todd A. Fehniger**[1]

[1]Washington University School of Medicine, Saint Louis, MO

[2]Medical University of South Carolina, Charleston, SC

[3]University of Minnesota, Minneapolis, MN

[4]Ohio State University, Columbus, OH

[5]ImmunityBio, Culver City, CA

Abstract

Purpose: N-803 is an IL-15 receptor superagonist complex, designed to optimize in vivo persistence and trans-presentation, thereby activating and expanding natural killer (NK) cells and CD8+ T cells. Monoclonal antibodies (mAb) direct FcR-bearing immune cells, including NK cells, to recognize and eliminate cancer targets. The ability of IL-15R agonists to enhance tumor-targeting mAbs in patients has not been previously reported.

Experimental Design: Relapsed/refractory indolent Non-Hodgkin's lymphoma patients were treated with rituximab and intravenous or subcutaneous N-803 on an open-label, dose-escalation phase 1 study using a 3+3 design (NCT02384954). Primary endpoint was maximum tolerated dose. Immune correlates were performed using multidimensional analysis via mass cytometry and

Correspondence: Todd A. Fehniger, Washington University, 660 S Euclid Ave, Campus Box 8007, St. Louis MO, 63110. Fax: 314.362.9333, Phone: 314.362.5658, tfehnige@wustl.edu.

Authors' Contributions: Conceptualization: T.A.F., A.D.R, J.L., M.M.B.E. Clinical trial design- T.A.F., A.D.R, J.L. Development of methodology and analysis design: A.A.P. J.A.F., T.A.F., M.M.B.E., M.M., O.L.G., M.G. F.G. Acquisition of data and clinical trial enrollments: E.M., M.F., T.S., M.B.H., J.A.W., J.A.F., M.M., M.M.B.E., N.L.B., B.T.H., V.B., B.K., A.F.C., C.M., N.M.S., K.M. ,N.E. Analysis and interpretation of data: T.A.F., J.A.F., A.A.P., M.B.H., M.M.B.E., N.D.M., F.G., Writing of manuscript: T.A.F., J.A.F. Study supervision: T.A.F., A.A.P., J.L., A.D.R, P. S-S. Editing and approval of final version of manuscript: All authors.

Conflict of Interest Statement: This clinical trial was supported by ImmunityBio (previously Altor BioScience). ADR, JL, and PS-S are employees or have financial interest in ImmunityBio. TAF has consulted for Nektar, Wugen, Indapta, Kiadis, Orca Bio, and has received research funding from ImmunityBio, Affimed, and Compass Therapeutics. BK has received research funding and consulting fees from Roche, Genentech, and Celgene. NMS has received research funding from Verastem Pharmaceuticals, Corvus Pharmaceuticals, Innate Pharmaceuticals, Bristol Myers Squibb, Genetech/Roche, Celgene and consulted for Kiowa Hakka Kirin, C4 Therapeutics, Karyopharma Therapeutics. NE has received funding from Verastem-Speaker's Bureau and Pharmacyclics-Honoraria. JAF has pending patents (WO 2019/152387, US 63/018,108) unrelated to the present work that are licensed to Kiadis, and a monoclonal antibody unrelated to the present work licensed to EMD Millipore. MBH is a co-inventor on a patent (US2010/0159594A1). MMBE is a consultant and has equity interest in Wugen, and may receive royalty income based on a technology developed by TAF and MMBE and licensed by Washington University to Wugen. MMBE has received travel funds from Fluidigm. All other authors have no conflicts of interest to report.

cellular indexing of transcriptomes and epitopes by sequencing (CITE-seq) which simultaneously measures protein and single-cell RNA expression.

Results: This immunotherapy combination was safe and well-tolerated and resulted in durable clinical responses including in rituximab-refractory patients. Subcutaneous N-803 plus rituximab induced sustained proliferation, expansion, and activation of peripheral blood NK cells and CD8 T cells, with increased NK cell and T cells present 8 weeks following last N-803 treatment. CITE-seq revealed a therapy-altered NK cell molecular program, including enhancement of AP-1 transcription factor. Further, the monocyte transcriptional program was remodeled with enhanced MHC expression and antigen-presentation genes.

Conclusions: N-803 combines with mAbs to enhance tumor-targeting in patients, and warrants further investigation in combination with immunotherapies.

INTRODUCTION

Immunotherapy is a rising modality in cancer therapeutics, harnessing concepts from immunology to enhance, trigger, or rescue immune responses against malignant targets. Established immunotherapies include engineered therapeutic monoclonal antibodies (mAbs), such as the anti-CD20 mAb rituximab, which targets endogenous Fc-receptor bearing immune cells, including natural killer (NK) cells, to B cell malignancies.(1) More recent successes in a variety of cancers have been the translation of anti-PD-1/PD-L1 and anti-CTLA-4 immune checkpoint blockade, which release induced brakes on tumor-reactive T cells.(2) Recently, complementary immunotherapy approaches utilizing cytokine receptor agonists are being tested as single-agents and in combination with immunotherapies to potentiate immune cell survival and function against cancer cells.(3) Currently, the use of this class of drugs is limited by adverse side-effects including fevers and chills, hypotension, and expansion of suppressive regulatory T cells (Tregs).(4-6) To address this unmet need in cancer immunotherapy, a new class of immune therapy biologics seeks to overcome these hurdles via innovative protein engineering, led by IL-15 receptor (IL-15R) agonists.

IL-15 is a key cytokine for the development, survival, and function of NK cells.(7) Recent in vitro and in vivo work demonstrated the ability of IL-15 to prime non-cytotoxic $CD56^{bright}$ NK cells to become anti-tumor effectors, a function previously believed to be largely restricted to the $CD56^{dim}$ NK cell subset.(8) IL-15 also plays a key role in supporting memory CD8+ T cells, thus augmenting two types of anti-tumor effector lymphocytes.(9) In vivo, IL-15 is trans-presented by IL-15Rα from accessory cells such as monocytes/macrophages and dendritic cells to ligate the IL-2/15Rγβ heterodimer expressed on NK and T cells, resulting in activation of multiple signaling pathways, and hence multiple anti-tumor functions.(9) Although IL-15 and IL-2 share signaling components, including the beta (CD122) and gamma chain (CD132), they have divergent effects, with IL-2 promoting Treg expansion.(10) Initial pioneering studies tested *E. coli*-derived recombinant human (rh)-IL-15, which demonstrated immune modulation in patients. However, rhIL-15 has a short half-life and dose levels that modulated immune cells were limited by unacceptable adverse events (AE).(4) N-803 (formerly ALT-803) is an IL-15R super agonist complex with a prolonged in vivo half-life, physiologic trans-presentation, and accumulation in secondary lymphoid tissues.(11) The initial study of N-803 in patients with hematologic malignancies

who relapsed after hematopoietic cell transplantation (HCT) demonstrated safety and modulation of immunity by N-803 but modest single agent clinical activity.(12)

We hypothesized that N-803 synergizes with the anti-CD20 lymphoma-targeting mAb rituximab to promote anti-lymphoma immune responses, which was supported by pre-clinical models.(13) To test this hypothesis, we designed a clinical trial combining N-803 with rituximab for patients with relapsed/refractory (rel/ref) indolent NHL (iNHL). Here, we report the safety, pharmacokinetics (PK), anti-lymphoma activity, and immunologic effects in the phase 1 study cohort.

MATERIALS & METHODS

Study design

Patients were treated on an open-label, multi-center (Washington University, University of Minnesota, Medical University of South Carolina), dose-escalation Phase 1 study registered on clinicaltrials.gov (NCT02384954) using a 3+3 design. Patients were enrolled beginning April 17, 2015 and ending July 23, 2017. Clinical data was analyzed by individual site investigators (TAF, BH, VB, NE) and verified and summarized by ImmunityBio; all authors had access to primary clinical trial data. PFS, OS, and duration of response of all treated patients was be assessed at least every three months during years 1 and 2, every 4 months during year 3, and then every 6 months (+/− 2 months) during years 4 and 5 from the start of study treatment, or through the point designated as the end of the study follow up (5 years). Information about disease response assessments and other therapies (chemotherapy, surgery, radiation therapy, other investigational treatment) received after discontinuation or completion of study treatment will be collected as available during the follow-up period. Patients with iNHL (follicular lymphoma, marginal zone lymphoma, small lymphocytic lymphoma, lymphoplasmacytic lymphoma) that were rel/ref after ≥2 prior lines of therapy were eligible. Patients were considered anti-CD20 mAb refractory if they progressed on anti-CD20 mAb therapy or within 6 months of their last dose of anti-CD20 mAb. Treatment consisted of IV rituximab 375 mg/m^2 and IV or SQ N-803 (in increasing dosing cohorts of 1, 3, 6, 10, 15, 20 μg/kg) on days 1, 8, 15, and 22 of cycle 1, followed by a rest period, and then consolidation with 4 additional treatments on days 78, 134, 190, and 246 (total of 8 treatments). For the initial 3 IV cohorts, rituximab was administered on day 1, and N-803 on day 2. Responses were assessed using the 2007 IHP criteria with assessment modifications to incorporate indeterminate response (IR) criteria.(14,15) The primary endpoints for the Phase 1 cohort was determination of the maximum tolerated or tested dose of N-803 and the recommended phase 2 dose (RP2D). Adverse events (AEs) were monitored and graded using the NCI CTCAE v4.0. Samples were collected for immune cell number and phenotyping pre-therapy (C1D1) and days 2, 5, 8, 15, 22, 23, and 26 of cycle 1, and days 78, 79, and 82 of the first consolidation cycle. Serum for cytokine and PK analysis was collected pre-therapy (0 minutes), and after N-803 at 30 minutes, 2 hours, 6 hours (C1D1) and days 2, 5, and 8.

Study Approval.

This clinical trial was approved at participating institutions IRBs and was conducted in accordance with recognized ethical guidelines (Declaration of Helsinki), and all patients provided written informed consent prior to study evaluation and treatment.

N-803 and cytokine measurements

Immunogenicity, N-803, IL-6, and IFNγ serum measurements were conducted as previously described.(12)

Flow Cytometry and Mass Cytometry

Patient PBMC were stained as previously described (Supp. Methods).(16) Absolute cell count of flow cytometry measured cell populations were only performed when absolute lymphocyte counts were available. Mass cytometry was performed (Table S1) on thawed patient PBMC as previously described.(12) Data were collected on a Helios mass cytometer (Fluidigm) and analyzed using Cytobank.(17)(18) Briefly, for each individual donor, cell subsets were identified using viSNE (v1, Table S1). These individually viSNE-gated subsets were then assessed. CD8 and CD4 T cells were assessed with an additional viSNE (v2), and subsets therein gated using unbiased FlowSOM analysis (Table S1, using all events, 36 clusters, 6 Metaclusters, 10 iterations, random seed, RRID:SCR_016899).(19)

CITE-seq Sample and Data Processing

PBMC were thawed in batch (Batch 1: 15, Batch 2: 16 & 17) and mixed with 5% murine spleen cells where indicated (Batch 2), and stained with oligonucleotide-tagged antibodies (ADTs) (Table S2, Supp. Methods). Following sequencing, FASTQ files were aligned to a custom genome consisting of the GRCh38 and mm10 reference and all patients and timepoints were aggregated using CellRanger (default settings, v.3.0.1; RRID:SCR_017344), and the resulting matrix was imported into the *R*-based package, Seurat (v.3.1/3.2; RRID:SCR_016341)(20-22) for normalization, batch-correction, clustering, visualization, and differential expression.(23) NK cells from patients 027-016 & 027-017 were imported into CiteFuse (RRID:SCR_019321) for clustering and UMAP projection using all ADTs and variable genes were selected for clustering using default settings.(24) For gene ontology analysis, we utilized *clusterprofiler* (RRID:SCR_016884). (25)

Statistics

Differential expression analysis was conducted in either R v 3.5/6 (RRID:SCR_001905), GraphPad Prism (v7/8) (RRID:SCR_002798), or SAS (v 9.4, SAS Institutes, Cary, NC; RRID:SCR_008567) with the appropriate parametric or non-parametric test as listed in the figure legend. For specific immune correlates as described in the figure legends, statistical analyses were performed comparing pre-treatment (D1) to the peak value for each variable within the time frames as indicated in the figures. For these analyses, the over-time changes were assessed using linear mixed models and post-hoc multiple comparisons for the differences between specific time-points of interest were only performed on those biomarkers that were significant in the overall test for improved control of the familywise

error rate. A logarithm transformation was applied to the absolute cell counts to better satisfy the normality and homoscedasticity assumptions.

Data Sharing Statement

Raw sequencing files will be available in dbGaP under accession phs001229 to qualified investigators at the time of publication. Clinical data will be deposited at clinicaltrials.gov in accordance with guidelines. For all other data requests, contact tfehnige@wustl.edu.

RESULTS

Patient characteristics and study therapy

Patients with rel/ref iNHL were enrolled in two sequential N-803 cohorts: intravenous (IV) (N=9 total; N=3 at each of 1, 3, and 6 μg/kg) and subcutaneous (SQ) (N=12 total; N=3 at each of 6, 10, 15, and 20 μg/kg) for a total of 21 patients (Fig. 1A, Table 1). Most patients had follicular lymphoma (FL) (76%), with a median of 2 (range 1-7) prior treatments, a median time from last prior anti-CD20 therapy to study therapy of 25 (range 1-134) months, and 5 patients were refractory to their last anti-CD20 mAb containing regimen. For the FL patients, 94% of patients had intermediate or high-risk Follicular Lymphoma International Prognostic Index (FLIPI) category. For study therapy, a standard dose and schedule of rituximab (375 mg/m^2) was chosen,(26) to allow comparison to historical clinical trials of single-agent rituximab, comprised of 4 weekly doses, followed by consolidation with 4 additional doses every two months (Fig. 1A). N-803 was administered on the same schedule as rituximab at patient-specific doses. No patients discontinued therapy due to a treatment-related AE.

Safety, tolerability, and serum cytokines

Patients in the N-803 IV cohort encountered grade 1-2 AEs, including a high frequency of fever and chills, typically occurring within 4 hours of the IV injection that responded to supportive care measures (Table 2). Correlative laboratory analysis of the PKs of N-803 revealed that the IV cohort patients had an early high C_{max} with near complete clearance within 24 hours (Fig. S1A). This coincided with elevations in both serum IFN-γ and IL-6, suggesting that IV N-803 was triggering acute cytokine release, responsible for the fever and rigors. While these were not dose-limiting, they were concerning for prolonged clinical dosing schedules, and a second cohort was initiated via the SQ route. Patients who received SQ N-803 uniformly experienced an injection site reaction consisting of non-painful erythema, warmth, and edema, which peaked at 7-10 days post-injection, and resolved with minimal supportive measures by two weeks. Patients also experienced fevers and chills, but these were transient and occurred 2-3 days after the SQ injection, resolving with supportive measures. Consistent with this change in constitutional symptoms based on N-803 route of administration, PK analysis revealed a lower C_{max} and prolonged serum concentration of N-803 following SQ administration, with minimal elevations in IFN-γ and IL-6 (Fig. S1B). Grade 3 non-hematologic toxicities in the SQ cohort were transient and included fever (N=1), hypertension (N=2), and hyperglycemia (N=1). Overall, the combination of rituximab and N-803 was well tolerated, without treatment-related grade 4 or 5 AEs (Table 2). Immunogenicity testing was also performed on Days 1, 22, and week 11 and

demonstrated no evidence of anti-N-803 antibodies developing in these patients at all time points (Table S3). Based on the dose escalation and PK, the recommended phase 2 dose was 15 or 20 ug/kg via the SQ route.

Clinical Response

Overall response rate (ORR) for the combined IV and SQ cohorts across all doses and CD20 mAb refractory status was 57% (12/21), with 44% (4 of 9) in the IV and 67% (8 of 12) in the SQ cohort. The majority of patients experienced reductions in the size of their lymph nodes (Fig. 1B). For patients with anti-CD20 mAb sensitive disease, the ORR in the IV cohort was 43% (3 of 7) and in the SQ cohort was 78% (7 of 9). In the SQ cohort, 7 of 7 (100%) responses were complete remissions (CR). Moreover, patients in the SQ cohort had prolonged stable disease (SD) and conversion of SD and/or partial response (PR) to CR with a prolonged duration without progression (8 of 12 patients without progression at 18-24 months) (Fig. 1C). In the SQ cohort, 6/7 CRs occurred at either the 1st (11 weeks) or 2nd evaluation (40 weeks). In the IV cohort, CR responses occurred following the 2nd evaluation and as late as 18 months follow-up. For the 5 patients with anti-CD20 mAb refractory disease in both IV and SQ cohorts, the ORR was 2 of 5 (40%) with 1 CR, 1 PR, 1 SD, and 2 PD (Fig. 1C, Fig. S1C). The PR and SD are ongoing in the SQ patients at > 18 months (Fig. 1C). The SQ cohort patient with PD was highly refractory, having received 5 prior lines of therapy.

N-803 plus rituximab induces expansion, activation, and modulation of NK cells

Here, we focused our correlative immunology on patients treated with 15 and 20 ug/kg SQ of N-803 because they had a similar PK profile (Fig. S1B) and relevant as the RP2D. Weekly SQ N-803 combined with rituximab resulted in a marked expansion in the frequency of total PB NK cells as assessed using multidimensional mass cytometry (Fig. 1D-F), with no significant change observed in the overall frequency of CD4+ or CD8+ T cells. The substantial increase in PB NK cells was confirmed using flow cytometry (Fig. 2A-E). This increase occurred early (days 5-15 of therapy) and was maintained throughout the 4 weeks of induction (days 22-27). Absolute NK cell counts remained elevated at D78, 8 weeks after the last N-803 dose (Fig. 2E). NK cell proliferation was increased, with ≥95% of NK cells expressing the cell cycle transit marker Ki-67 after the first dose of N-803 (Fig. 2F-H). This proliferative effect was maintained throughout induction as well, with Ki-67^{+} NK cells >50% when assessed at days 15 and 21 (prior to N-803 injections). The response of NK cells to N-803 was examined 8 weeks after induction at the time of the first consolidation therapy. Here, N-803 induced increases in Ki-67^{+} NK cells, comparable to the first dose of N-803, suggesting a prolonged administration schedule was feasible (Fig. 2I). As an indicator of functionality, significant upregulation of the cytotoxic protein granzyme B was observed following N-803 plus rituximab therapy (Fig. 2J).

To provide a multidimensional assessment of NK cells, the mass cytometry data was analyzed gating on the NK cell viSNE islands. NK cells demonstrated a marked change in their multidimensional phenotype at days 8 and 22 (Fig. 2K), which was driven by the activation marker CD38, and activating receptors NKp30 and NKp44 (Fig. 2L-M), and EOMES, a T-box transcription factor associated with NK cell functionality.(27-29) Thus,

N-803 in the presence of a therapeutic mAb resulted in a sustained expansion and alteration of the NK cell activation state following therapy.

N-803 plus rituximab induces activation, proliferation, and modulation of CD8+ T cells

We hypothesized that N-803 would also result in changes in the CD8+ T cell compartment. A modest increase in absolute CD8+ T cell numbers were observed at the later time points of N-803 induction and maintained 8 weeks after induction therapy at D78, while no change was observed in CD8+ T cell percentage (Fig. 3A-B). In addition, subsets of CD8+ T cells expressed Ki-67, at both early and later time points of N-803 induction, although at a lower peak frequency (~50%) than in NK cells (Fig. 3C-E, Fig. 2G-H). Using mass cytometry and viSNE to gate on major T cell subsets within PB lymphocytes, no changes in the overall frequency of naïve (T_N), effector (T_E), and central memory (T_{CM}) CD8+ T cells were observed as defined using FlowSOM clustering, however a subset of effector memory (T_{EM}) (MC2) was increased after N-803 administration (Fig. 3F). This metacluster was defined by high Ki67, CD38, HLA-DR, and TIM-3 expression along with intermediate expression of PD-1 ($p<0.05$) compared to the other T_{EM} subsets (Fig. 3G-I). However, by day 22 the CD8+ T cell profile had returned to a pre-therapy phenotype.

N-803 plus rituximab has minimal impact on CD4+ T cells and Tregs

Next, we examined the impact of N-803 plus rituximab therapy on CD4+ T cells. The frequency of CD4+ T cells did not increase over the course of N-803 induction therapy; however, there was a minimal but significant increase in overall CD4+ T cell numbers which persisted at D78 (Fig. S2A-D). This was accompanied by a minor increase in the percentage of Ki67+ CD4+ T cells with a mean peak of 22% at D2-15 (Fig. S2E-F). Clustering analysis on the CD4+ T cells in mass cytometry, revealed no significant changes in the FlowSOM identified metaclusters, indicating minimal phenotypic changes with N-803 and rituximab (Fig. S2G). There was a small increase in the frequency of CD4+ Tregs during the early phase of induction and immediately following the first dose of N-803 in consolidation, and a modest increase in Ki-67+ Tregs during the early phase of induction, but no change in absolute Treg numbers (Fig. S2H-L). Thus, while modest and of unclear biological significance, activation of a small fraction of CD4+ T cells was observed with N-803, consistent with established IL-15R biology.

Cellular Indexing of Transcriptomes and Epitopes (CITE) seq reveals changes in PBMC transcriptomes following N-803 plus rituximab therapy

To better understand the impact of N-803 plus rituximab, we performed CITE-seq(20) using a custom antibody panel designed for NK cells, which measures protein using barcode tagged antibodies (ADTs) while simultaneously performing single-cell RNA-seq (scRNAseq) on PBMC samples at day 1 (pre-N-803, n=3), day 8 (n=2), and day 15 (n=3) (Fig. 4A, Fig. S3A-C). Distinct and shared impact of N-803 plus rituximab on NK cell subsets was evident (Fig. 4B-C, Fig. S3D). In $CD56^{bright}$ NK cells, a significant enrichment in Gene Ontology (GO) Biological Processes (BP) related to NF-kappaB and MAPK signaling, cytotoxicity, cell-adhesion, and proliferation was observed, while $CD56^{dim}$ NK cells were enriched for leukocyte activation and both NK subsets were enriched for cytokine-related BP (Fig. S3D). These changes in BP corresponded to increased expression

of granzymes (*GZM*) *A*, *B*, *K*, and *H*, and perforin (*PRF1*), and the T-box transcription factor, T-BET (*TBX21*) in CD56^{bright} NK cells, providing evidence of in vivo priming (Fig. 4B). CD56^{dim} NK cells had increased expression of chemotaxis genes (*CCL3*, *CXCR4*), *FOS* and *CEBPB* transcription factors, and interferon-inducible genes (*IFITM3*, *IFI6*) (Fig. 4C). In agreement with our cytometry data, we observed increased *CD38* RNA (Fig. 4B-C) and protein (Fig. S3E). NK cell molecular changes were evident by D8 with no further differentially expressed genes in CD56^{bright} and only two differentially expressed genes in CD56^{dim} (*CCL4L2*, *AREG*) between D8 and D15, suggesting that N-803 alters the NK transcriptome after the first dose.

Identification of KIR+ and terminally mature (CD57+) CD56^{dim} NK cell subsets with scRNAseq has been hindered by high transcript drop-out rate of current technologies, resulting in poor enrichment for CD57 (*B3GAT1*) and KIRs. To address this, we performed similarity network fusion implemented in CiteFuse(24,30), re-clustering NK cells using both protein and RNA (Fig. 4D-E). Unsupervised clustering revealed increased heterogeneity of CD56^{dim} NK, but only one cluster of CD56^{bright} NK, accurately recapitulating known biology of NK cell maturation (Fig. 4D & 4F, S3F-G, S4A-B).(31) In addition, CiteFuse uncovered a conserved decrease in CD57+ NK cells, as well as patient-specific changes in CD56^{dim} NK cell subsets, which may represent a repair of a dysfunctional CD56^{dim} compartment in patient 027-016 (Fig. S4A). Transcriptional changes were enriched in subsets of CD56^{dim} NK cells, including upregulation of AP-1 subunits *JUN* and *FOS,* and *CD69* (Fig. 4G, S4C-D), suggesting that N-803 and rituximab may preferentially activate specific CD56^{dim} NK cell subsets in vivo. In addition, IL-15 pathway gene expression changes were driven by only one patient indicating that N-803 may have both shared and individual responses (Fig. S4D).

Evidence of augmented HLA-DR and CD38 was found in CD8+ T_{EM}, consistent with mass cytometry findings (Fig. S4E-F). In γδ T cells, a significant increase in the expression of cytotoxicity genes (*GNLY*, *GZMB*, *GZMH*, *NKG7*), transcription factors (*TBX21*, *JUN*), secreted proteins (*FGFBP2*, *CCL5*), and MHC Class II (*HLA-DRB1*, *HLA-DPA1*, *CD74*), were observed at D15 (Fig. 4H). In the monocyte compartment, striking shifts in the *t*SNE space of CD14 monocytes was accompanied by a significant decrease in the proportion of CD14 monocytes (Fig. S4G). Similarly, a significant decrease in CD16+ monocytes was evident (Fig. 4I). Gene expression changes driving this marked shift included increased type 1 interferon and IFNγ inducible genes (Fig. S4H, Fig. 4J), humoral immune responses, complement activation (*C1QA, C1QB, C1QC*), antigen processing and presentation (*HLA-DPA1*, *HLA-DPB1*, *HLA-DQA1*, *HLA-DQB1*, *HLA-DRA*, *HLA-DRB1*, *CD74*), and antibody-responses (*FCGR1A*) (Fig. 4J).

DISCUSSION

Here we report the first-in-human clinical trial of an IL-15R agonist in combination with a tumor-targeting mAb. Administration of SQ N-803 with rituximab had an excellent safety profile and demonstrated prolonged PFS and a 78% CR rate in rituximab-sensitive patients. Correlative immunology in the PB revealed distinct activation signatures of CD56^{bright} and CD56^{dim} NK cells, including priming of CD56^{bright} NK cells, along with increased NK

proliferation which contrasts with previous study following single-agent rituximab.(32) Within the T cell compartment, CD8+ T_{EM} exhibited marked but transient activation and expansion characterized by high expression of CD38 and HLA-DR. Using scRNAseq, we observed γδ T cell activation along with a profound change in monocytes and enhanced antigen presentation and type I interferon genes. These studies support the mechanism of action of N-803 as an activator of NK and CD8+ T cells, and provide insights into the potential for broad immune modulation with this novel combination therapy.

As IV rhIL-15 promotes NK and CD8+ T cell proliferation, but results in unacceptable AE, several IL-15R agonist drugs have since been developed and translated into the clinic to mitigate these barriers.(6) N-803 has been the pioneer in this class of drugs, and was proven to have a prolonged in vivo half-life, while maintaining the ability to stimulate NK and CD8+ T cells(11,33,34), and is currently being investigated in several cancer types including NSCLC where it has demonstrated efficacy in difficult to treat patient populations and an excellent safety profile.(35) Here we report that SQ administration of N-803 is well-tolerated, and identify 15-20 μg/kg N-803 as the RP2D doses for future study in this clinical setting.(12,35,36) Clinical responses were observed in 78% of SQ rituximab-sensitive patients warranting further clinical study. In comparison, single agent rituximab has an ORR of 40-53% and a CR rate of 11-18%.(26,37,38) We observed responses in 2 of 5 rituximab-refractory patients, further supporting the importance of N-803 in the observed responses. It is intriguing to postulate that N-803 may restore iNHL responses when used in conjunction with a tumor targeting mAb, which should be addressed in larger phase 2 trial cohorts.

N-803 is currently being investigated in several cancer clinical trials as a combination therapy including with gemcitabine and in combination with adoptive NK cell therapy. Based on this study, broad testing of N-803 in concert with cancer-targeting mAbs is warranted. Thus, this class of IL-15R agonists has the potential to transform immunotherapy for multiple cancer types.

Distinct from the focused monitoring of previously reported N-803 trials(12,35), we applied scRNAseq to comprehensively define N-803 and rituximab mediated alterations of immune cell molecular programs revealing unexpected immune modulation. For example, we demonstrate activation of antigen-presentation genes in CD16 monocytes and type 1 IFN and IFNγ family genes, suggesting that immune cross talk between NK cells, T cells, and monocytes occur. Further, the decrease in blood monocytes following therapy coupled with the increased expression of *FCGR1A*, may be indicative of trafficking to the site of the lymphoma where the monocytes mediate antibody-directed effects and T cell activation. The enhanced antigen presentation program and MHC class II expression suggests potential utility as an adjunct to vaccines. These findings suggest that N-803 may simultaneously enhance innate and adaptive immune responses to lymphoma. Future studies correlating the magnitude of immune changes within monocytes, T cells, and NK cells with clinical response will be informative to understanding the mechanisms behind N-803 and rituximab mediated clinical outcomes.

Consistent with previous work on single-agent N-803 post-HCT(12), NK cells exited the circulation immediately following N-803 treatment, and then rapidly expanded with

sustained Ki67 expression. Previous work on N-803 has demonstrated increased NK cell localization in the lymph node shortly after N-803 administration, providing a potential explanation for the transient decrease in NK cells observed in this study.(39) Future studies will be of interest to identify the prevalence and phenotypic changes of immune cells within the lymph nodes following N-803 and anti-CD20 mAbs, particularly as this relates to lymphoma immune surveillance. Our findings add to prior work on N-803 demonstrating here that NK and CD8+ T cell total counts remain elevated 8 weeks after N-803 treatment, suggesting a prolonged effect of N-803 on the immune milieu in lymphoma patients. This finding may represent restoration of blood lymphocyte counts by N-803, as lymphopenia is frequently present in lymphoma patients and is adversely correlated with poor clinical outcome.(40)

Using scRNAseq profiling, we find cytotoxic effector molecules increased (*GZMA*, *GZMB*, *GZMK*, *GZMH*, *PRF1*, *GNLY*) in $CD56^{bright}$ NK cells consistent with previous *in vitro* reports on IL-15 priming of $CD56^{bright}$ NK cells. These findings stand in contrast to previous work in single-agent rituximab treated lymphoma patients, where rituximab-treated patients had decreased NK cell counts; however, future in depth studies comparing the effect of single-agent anti-CD20 mAbs and N-803 are required to better elucidate the contribution of each therapy and are being accrued as part of the larger ongoing phase 2 trial.(32)

Further, CITE-seq revealed a significant change in the transcription factor profile of N-803 expanded NK cells, with AP-1 member, *JUN*, and *CEBPB* significantly increased across most NK clusters. These data lead to important, novel molecular characterization of NK cells in vivo, and generate hypotheses related to key molecular changes that occur following IL-15 administration. The addition of cell-surface protein to scRNAseq data in CITE-seq overcomes many of the current technical limitations of scRNAseq for NK cells, facilitating the identification of CD57+ NK cells as a subset significantly decreased following treatment, potentially due to N-803 induced proliferation of other NK cell subsets, as CD57+ NK cells are reported to have low proliferative potential.(41) Furthermore, CiteFuse revealed increased heterogeneity in the N-803 and rituximab changes in $CD56^{dim}$ NK cell populations but not $CD56^{bright}$, indicating that $CD56^{dim}$ NK cell heterogeneity is not captured by scRNAseq alone. Additionally, we observed increased differences in the proportion of $CD56^{dim}$ clusters across patients, likely driven by known individual differences in KIR repertoires.(42,43) The CITE-seq approach will be critical for comprehensively evaluating NK cells at the single cell level in response to immunotherapy.

Here we report preferential activation of CD8+ T_{EM} subsets consistent with prior publications in humans and macaques.(12,44,45) This effect may be due to the increased sensitivity of human CD8+ T_{EM} to IL-15, consistent with increased IL-15 receptor expression on T_{EM}.(45) In contrast, in mice, IL-15 activates and expands T_{CM} to a greater degree than T_{EM}, likely due to increased expression of CD122 on murine T_{CM}.(46,47) Together, these studies suggest a gradient of IL-15 responsiveness across T cell subsets driving IL-15 activation and proliferation responses.

Here, we demonstrate that a new combination immunotherapy of the IL-15R agonist N-803, and the tumor targeting antibody, rituximab, is safe and shows preliminary clinical activity

in a phase 1 trial of rel/ref iNHL patients. Using multi-dimensional mass cytometry and CITE-seq, we define protein and transcriptional changes, demonstrating remodeling of iNHL patient immune landscapes by promotion of an activation signature in nearly all main immune cell lineages including NK cells, CD8+ T_{EM}, γδ T cells, and CD14 and CD16 monocytes. These findings warrant additional investigations on the efficacy of N-803 and anti-CD20 mAbs in ongoing trials for iNHL (NCT02384954) and the testing of N-803 in combination with other therapeutic antibodies in additional cancers. Extended studies on the long-term effects of N-803 and anti-CD20 mAbs on the NHL immune environment are currently underway as part of the phase 2 trial.

Supplementary Material

Refer to Web version on PubMed Central for supplementary material.

Acknowledgments:

We would like to acknowledge the patients and clinical lymphoma teams for making this study possible. We would like to acknowledge the Siteman Flow Cytometry (Bill Eades), Immune Monitoring Lab (Stephen Oh), and McDonnell Genome Institute (Catrina Fronick, Bob Fulton, Alex Paul).

Funding:

The clinical trial was supported by R44 CA195812 and ImmunityBio. NIH T32 HL007088 (J.A.Wagner, J.A.Foltz), SPORE in Leukemia P50CA171963 (M.M.Berrien-Elliott, A.F.Cashen, T.A.Fehniger), K12CA167540 (M.M.Berrien-Elliott), R01CA205239 (T.A.Fehniger), American Association of Immunologists Intersect Fellowship Program for Computational Scientists and Immunologists (J.A.Foltz, A.A.Petti, T.A.Fehniger); MGI Pilot Grant (T.A.Fehniger), Jamie Erin Follicular Lymphoma Research Fund (T.A.Fehniger). This work was also supported by the NCI CCSG P30 C091842 (Siteman Cancer Center).

References

1. Cheson BD, Leonard JP. Monoclonal Antibody Therapy for B-Cell Non-Hodgkin's Lymphoma. N Engl J Med. 2008;359:613–26. [PubMed: 18687642]
2. Sharma P, Allison JP. The future of immune checkpoint therapy. Science (80-). 2015;348:56–61.
3. Conlon KC, Miljkovic MD, Waldmann TA. Cytokines in the Treatment of Cancer. J Interf Cytokine Res. Mary Ann Liebert Inc.; 2019;39:6–21.
4. Conlon KC, Lugli E, Welles HC, Rosenberg S a, Fojo AT, Morris JC, et al. Redistribution, Hyperproliferation, Activation of Natural Killer Cells and CD8 T Cells, and Cytokine Production During First-in-Human Clinical Trial of Recombinant Human Interleukin-15 in Patients With Cancer. J Clin Oncol. 2015;33:74–82. [PubMed: 25403209]
5. Miller JS, Morishima C, McNeel DG, Patel MR, Kohrt HEK, Thompson JA, et al. A first-in-human phase I study of subcutaneous outpatient recombinant human IL15 (rhIL15) in adults with advanced solid tumors. Clin Cancer Res. American Association for Cancer Research Inc.; 2018;24:1525–35. [PubMed: 29203590]
6. Waldmann TA. The Shared and Contrasting Roles of IL2 and IL15 in the Life and Death of Normal and Neoplastic Lymphocytes: Implications for Cancer Therapy. Cancer Immunol Res. American Association for Cancer Research Inc.; 2015;3:219–27. [PubMed: 25736261]
7. Fehniger TA. Mystery Solved: IL-15. J Immunol. 2019;202:3125–6. [PubMed: 31109944]
8. Wagner J A, Rosario M, Romee R, Berrien-Elliott M,M, et al. CD56bright NK cells exhibit potent antitumor responses following IL-15 priming. J Clin Invest. 2017;127:4042–58. [PubMed: 28972539]
9. Fehniger TA, Caligiuri MA. Interleukin 15: biology and relevance to human disease. Blood. 2001;97:14–32. [PubMed: 11133738]

10. Waldmann TA. The biology of interleukin-2 and interleukin-15: implications for cancer therapy and vaccine design. Nat Rev Immunol. 2006;6:595–601. [PubMed: 16868550]
11. Rhode PR, Egan JO, Xu W, Hong H, Webb GM, Chen X, et al. Comparison of the Superagonist Complex, ALT-803, to IL15 as Cancer Immunotherapeutics in Animal Models. Cancer Immunol Res. 2016;4:1–13. [PubMed: 26729616]
12. Romee R, Cooley S, Berrien-Elliott MM, Westervelt P, Verneris MR, Wagner JE, et al. First-in-human phase 1 clinical study of the IL-15 superagonist complex ALT-803 to treat relapse after transplantation. Blood. 2018;131:2515–27. [PubMed: 29463563]
13. Rosario M, Liu B, Kong L, Collins L, Schneider SE, Chen X, et al. The IL-15-based ALT-803 complex enhances Fc RIIIa-triggered NK cell responses and in vivo clearance of B cell lymphomas. Clin Cancer Res. 2016;22:596–608. [PubMed: 26423796]
14. Cheson BD, Pfistner B, Juweid ME, Gascoyne RD, Specht L, Horning SJ, et al. Revised Response Criteria for Malignant Lymphoma. J Clin Oncol. 2007;25:579–86. [PubMed: 17242396]
15. Cheson BD, Ansell S, Schwartz L, Gordon LI, Advani R, Jacene HA, et al. Refinement of the Lugano Classification lymphoma response criteria in the era of immunomodulatory therapy. Blood. 2016;128:2489–97. [PubMed: 27574190]
16. Romee R, Rosario M, Berrien-Elliott MM, Wagner JA, Jewell BA, Schappe T, et al. Cytokine-induced memory-like natural killer cells exhibit enhanced responses against myeloid leukemia. Sci Transl Med. American Association for the Advancement of Science; 2016;8(357):357:doi: 10.1126/scitranslmed.aaf2341.
17. Kotecha N, Krutzik PO, Irish JM. Web-based analysis and publication of flow cytometry experiments. Curr Protoc Cytom. 2010;Chapter 10:Unit10.17.
18. Diggins KE, Ferrell PB, Irish JM. Methods for discovery and characterization of cell subsets in high dimensional mass cytometry data. Methods. 2015;82:55–63. [PubMed: 25979346]
19. Van Gassen S, Callebaut B, Van Helden MJ, Lambrecht BN, Demeester P, Dhaene T, et al. FlowSOM: Using self-organizing maps for visualization and interpretation of cytometry data. Cytom Part A. 2015;87:636–45.
20. Stoeckius M, Hafemeister C, Stephenson W, Houck-Loomis B, Chattopadhyay PK, Swerdlow H, et al. Simultaneous epitope and transcriptome measurement in single cells. Nat Methods. Nature Publishing Group; 2017;14:865–8. [PubMed: 28759029]
21. Stuart T, Butler A, Hoffman P, Hafemeister C, Papalexi E, Mauck WM, et al. Comprehensive Integration of Single-Cell Data. Cell. Cell Press; 2019;177:1888–1902.e21. [PubMed: 31178118]
22. Butler A, Hoffman P, Smibert P, Papalexi E, Satija R. Integrating single-cell transcriptomic data across different conditions, technologies, and species. Nat Biotechnol. Nature Publishing Group; 2018;36:411–20. [PubMed: 29608179]
23. Petti AA, Williams SR, Miller CA, Fiddes IT, Srivatsan SN, Chen DY, et al. A general approach for detecting expressed mutations in AML cells using single cell RNA-sequencing. Nat Commun. Springer Science and Business Media LLC; 2019;10.
24. Kim HJ, Lin Y, Geddes TA, Yang JYH, Yang P. CiteFuse enables multi-modal analysis of CITE-seq data. Bioinformatics. 2020;36:4137–43. [PubMed: 32353146]
25. Yu G, Wang LG, Han Y, He QY. ClusterProfiler: An R package for comparing biological themes among gene clusters. Omi A J Integr Biol. Mary Ann Liebert, Inc.; 2012;16:284–7.
26. Ghielmini M, Schmitz SH, Cogliatti SB, Pichert G, Waltzer U, Fey MF, et al. Prolonged treatment with rituximab in patients with follicular lymphoma significantly increases event-free survival and response duration compared with the standard weekly x 4 schedule. Blood. 2004;103:4416–24. [PubMed: 14976046]
27. Simonetta F, Pradier A, Bosshard C, Masouridi-Levrat S, Chalandon Y, Roosnek E. NK Cell Functional Impairment after Allogeneic Hematopoietic Stem Cell Transplantation Is Associated with Reduced Levels of T-bet and Eomesodermin. J Immunol. The American Association of Immunologists; 2015;195:4712–20. [PubMed: 26438526]
28. Gill S, Vasey AE, De Souza A, Baker J, Smith AT, Kohrt HE, et al. Rapid development of exhaustion and down-regulation of eomesodermin limit the antitumor activity of adoptively transferred murine natural killer cells. Blood. 2012;119:5758–68. [PubMed: 22544698]

29. Zhang J, Marotel M, Fauteux-Daniel S, Mathieu A-L, Viel S, Marçais A, et al. T-bet and Eomes govern differentiation and function of mouse and human NK cells and ILC1. Eur J Immunol. 2018;48:738–50. [PubMed: 29424438]
30. Wang B, Mezlini AM, Demir F, Fiume M, Tu Z, Brudno M, et al. Similarity network fusion for aggregating data types on a genomic scale. Nat Methods. Nature Publishing Group; 2014;11:333–7. [PubMed: 24464287]
31. Björkström NK, Riese P, Heuts F, Andersson S, Fauriat C, Ivarsson M a, et al. Expression patterns of NKG2A, KIR, and CD57 define a process of CD56dim NK-cell differentiation uncoupled from NK-cell education. Blood. 2010;116:3853–64. [PubMed: 20696944]
32. Enqvist M, Jacobs B, Junlén HR, Schaffer M, Melén CM, Friberg D, et al. Systemic and Intra-Nodal Activation of NK Cells After Rituximab Monotherapy for Follicular Lymphoma. Front Immunol. 2019;10.
33. Han K ping, Zhu X, Liu B, Jeng E, Kong L, Yovandich JL, et al. IL-15:IL-15 receptor alpha superagonist complex: high-level co-expression in recombinant mammalian cells, purification and characterization. Cytokine. Elsevier Ltd; 2011;56:804–10. [PubMed: 22019703]
34. Xu W, Jones M, Liu B, Zhu X, Johnson CB, Edwards AC, et al. Efficacy and Mechanism-of-Action of a Novel Superagonist Interleukin-15: Interleukin-15 Receptor αSu/Fc Fusion Complex in Syngeneic Murine Models of Multiple Myeloma. Cancer Res. 2013;73:3075–86. [PubMed: 23644531]
35. Wrangle JM, Velcheti V, Patel MR, Garrett-Mayer E, Hill EG, Ravenel JG, et al. ALT-803, an IL-15 superagonist, in combination with nivolumab in patients with metastatic non-small cell lung cancer: a non-randomised, open-label, phase 1b trial. Lancet Oncol. 2018;19:694–704. [PubMed: 29628312]
36. Margolin K, Morishima C, Velcheti V, Miller JS, Lee SM, Silk AW, et al. Phase I Trial of ALT-803, A Novel Recombinant IL15 Complex, in Patients with Advanced Solid Tumors. Clin Cancer Res. American Association for Cancer Research; 2018;24:5552–61. [PubMed: 30045932]
37. Davis TA, Grillo-López AJ, White CA, McLaughlin P, Czuczman MS, Link BK, et al. Rituximab anti-CD20 monoclonal antibody therapy in non-Hodgkin's lymphoma: Safety and efficacy of re-treatment. J Clin Oncol. American Society of Clinical Oncology; 2000;18:3135–43. [PubMed: 10963642]
38. Leonard JP, Trneny M, Izutsu K, Fowler NH, Hong X, Zhu J, et al. AUGMENT: A Phase III study of lenalidomide plus rituximab versus placebo plus rituximab in relapsed or refractory indolent lymphoma. J Clin Oncol. American Society of Clinical Oncology; 2019. page 1188–99.
39. Webb GM, Molden J, Busman-Sahay K, Abdulhaqq S, Wu HL, Weber WC, et al. The human IL-15 superagonist N-803 promotes migration of virus-specific CD8+ T and NK cells to B cell follicles but does not reverse latency in ART-suppressed, SHIV-infected macaques. PLoS Pathog. 2020;16:1–23.
40. Ray-Coquard I, Cropet C, Van Glabbeke M, Sebban C, Le Cesne A, Judson I, et al. Lymphopenia as a prognostic factor for overall survival in advanced carcinomas, sarcomas, and lymphomas. Cancer Res. NIH Public Access; 2009;69:5383–91. [PubMed: 19549917]
41. Lopez-Vergès S, Milush JM, Pandey S, York V a, Arakawa-Hoyt J, Pircher H, et al. CD57 defines a functionally distinct population of mature NK cells in the human CD56dimCD16+ NK-cell subset. Blood. 2010;116:3865–74. [PubMed: 20733159]
42. Hsu KC, Liu X-R, Selvakumar A, Mickelson E, O'Reilly RJ, Dupont B. Killer Ig-Like Receptor Haplotype Analysis by Gene Content: Evidence for Genomic Diversity with a Minimum of Six Basic Framework Haplotypes, Each with Multiple Subsets. J Immunol. The American Association of Immunologists; 2002;169:5118–29. [PubMed: 12391228]
43. Wilson MJ, Torkar M, Haude A, Milne S, Jones T, Sheer D, et al. Plasticity in the organization and sequences of human KIR/ILT gene families. Proc Natl Acad Sci U S A. National Academy of Sciences; 2000;97:4778–83. [PubMed: 10781084]
44. DeGottardi MQ, Okoye AA, Vaidya M, Talla A, Konfe AL, Reyes MD, et al. Effect of Anti–IL-15 Administration on T Cell and NK Cell Homeostasis in Rhesus Macaques. J Immunol. The American Association of Immunologists; 2016;197:1183–98. [PubMed: 27430715]

45. Geginat J, Lanzavecchia A, Sallusto F. Proliferation and differentiation potential of human CD8+ memory T-cell subsets in response to antigen or homeostatic cytokines. Blood. American Society of Hematology; 2003;101:4260–6. [PubMed: 12576317]

46. Kokaji AI, Hockley DL, Kane KP. IL-15 Transpresentation Augments CD8 + T Cell Activation and Is Required for Optimal Recall Responses by Central Memory CD8 + T Cells . J Immunol. The American Association of Immunologists; 2008;180:4391–401. [PubMed: 18354159]

47. Osborn JF, Mooster JL, Hobbs SJ, Munks MW, Barry C, Harty JT, et al. Enzymatic synthesis of core 2 O-glycans governs the tissue-trafficking potential of memory CD8+ T cells. Sci Immunol. American Association for the Advancement of Science; 2017;2:13.

STATEMENT OF TRANSLATIONAL RELEVANCE

We report the first phase 1 clinical trial of an IL-15 receptor agonist (N-803) with a tumor-targeting antibody. N-803 plus the anti-CD20 monoclonal antibody, rituximab, was well-tolerated and induced a 78% CR rate in rituximab-sensitive iNHL patients with subcutaneous N-803. N-803 plus rituximab also induced prolonged responses in a subset of rituximab-refractory patients. Using high-dimensional mass cytometry and single-cell RNA-sequencing, we show for the first time that N-803 activates nearly all major immune cell lineages including natural killer cells, CD8+ T cells, and monocytes, with minimal changes in CD4+ T cells. These findings support the use of N-803 in combination with additional therapeutic antibodies, and other immunotherapy approaches, in lymphoma and other cancer types.

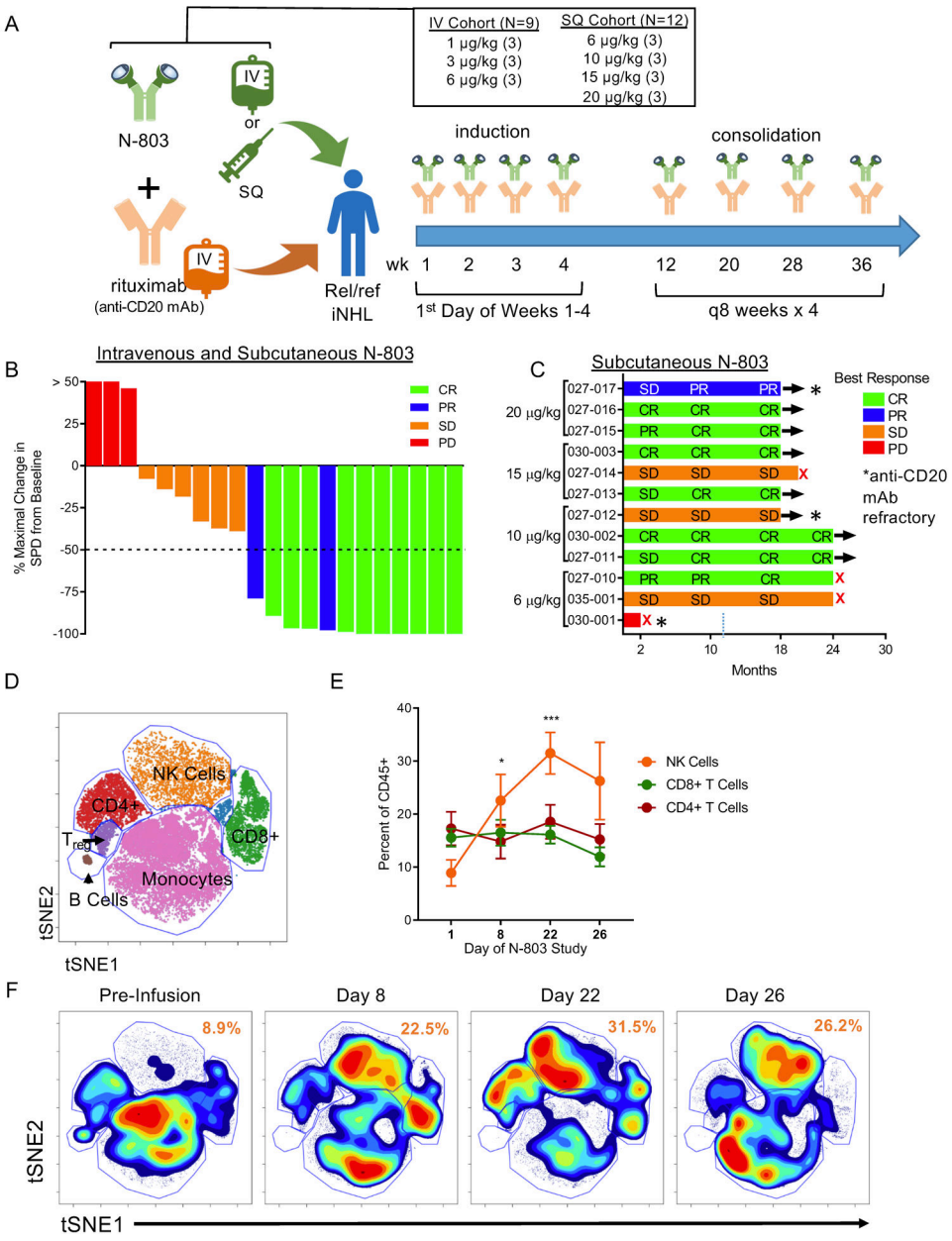

Figure 1. N-803 and Rituximab induce clinical responses and immune modulation in a Phase 1 trial.

A) Schematic of the phase 1 clinical trial and dosing regimens. B) Waterfall plot depicting the percent maximal change in the sum of the products of the greatest diameter (SPD) of the lymphoma tumor burden and the best clinical response for all patients in the IV and SQ cohort by color. n = 21 C) Swimmer plot for SQ N-803 patients depicting best clinical responses across follow-up by dose. n = 12. Red X denotes PD. * denotes rituximab-refractory patient. D) Representative *t*SNE visualization of major immune cell lineages in high-dimensional mass cytometry data. E) Percentage of NK, CD8+ T cells, and CD4+ T cells in patient PBMC pre-treatment (D1) and during N-803 and rituximab treatment (D8-22). Mean ± SEM depicted. n = 5, 3 independent experiments. 2-way ANOVA with

Dunnett's multiple comparison's test. F) Representative *t*SNE density plot of PBMC lineages across time. Numbers in orange denoting mean of NK cell percentages across time. * = $p < 0.05$, ** = $p \leq 0.01$, *** = $p \leq 0.001$, **** = $p \leq 0.0001$.

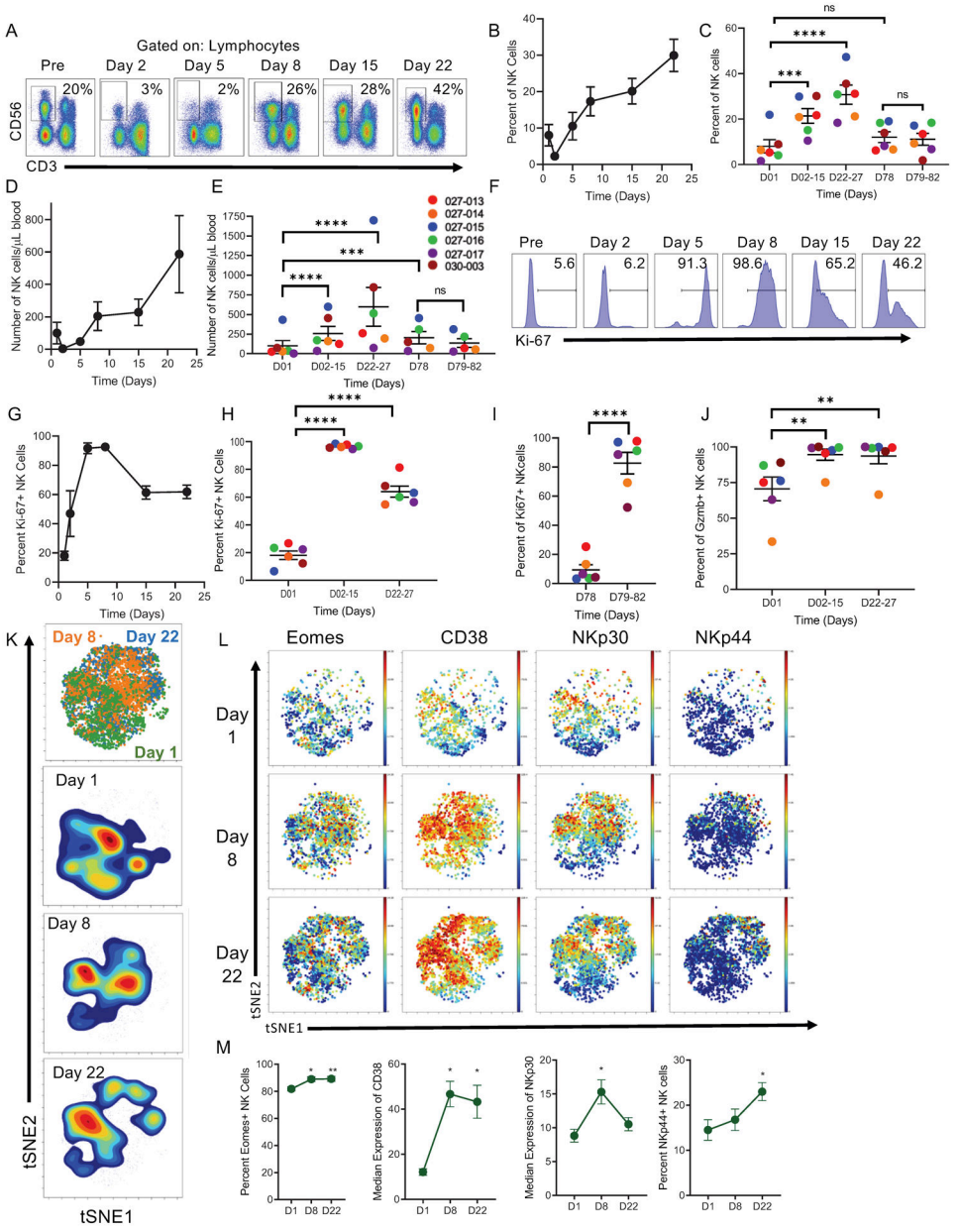

Figure 2. N-803 and rituximab induce activation, expansion, and proliferation of PB NK cells.

A) Representative Flow Cytometry plots of NK cells at each time points. Black box denotes NK cell gate, and numbers denote percent of NK cells in lymphocytes at each time point. B) Line graph and C) dot plot depicting the percentage of NK cells by time. D) Line graph and E) dot plot of absolute number of NK cells per μl of blood. F) Representative flow histograms of Ki-67 expression in NK cells at each time point. Numbers denote percent of Ki-67+ NK cells. G) Line graph and H-I) Dot plot of Ki-67+ NK cells at each time point during induction and consolidation. J) Dot Plot depicting percent of granzyme B+ NK cells by patient. Linear mixed model for all of the above. K) *t*SNE visualization and density plots gated on NK cells assessed by mass cytometry. L) Representative mass cytometry viSNE plots of Eomes, CD38, NKp30, and NKp44 expression in NK cells; blue- low expression,

red- high expression. Line graphs depicting M) percent of Eomes+, CD38 and NKp30 Median Expression, and NKp44+ NK cells. n = 5-6, ≥ 3 independent experiments. Friedman's test for NKp44 and Dunn's multiple comparisons, RM one-way ANOVA and Dunnett's multiple comparisons for all others. Mean ± SEM for all line and dot plots. Line graphs depict Mean ± SEM of values for all patients. Individual dots represent individual patients. Significance for mass cytometry comparisons $p < 0.05$, all others $p < 0.01$. * = $p < 0.05$, ** = $p \leq 0.01$, *** = $p \leq 0.001$, **** = $p \leq 0.0001$.

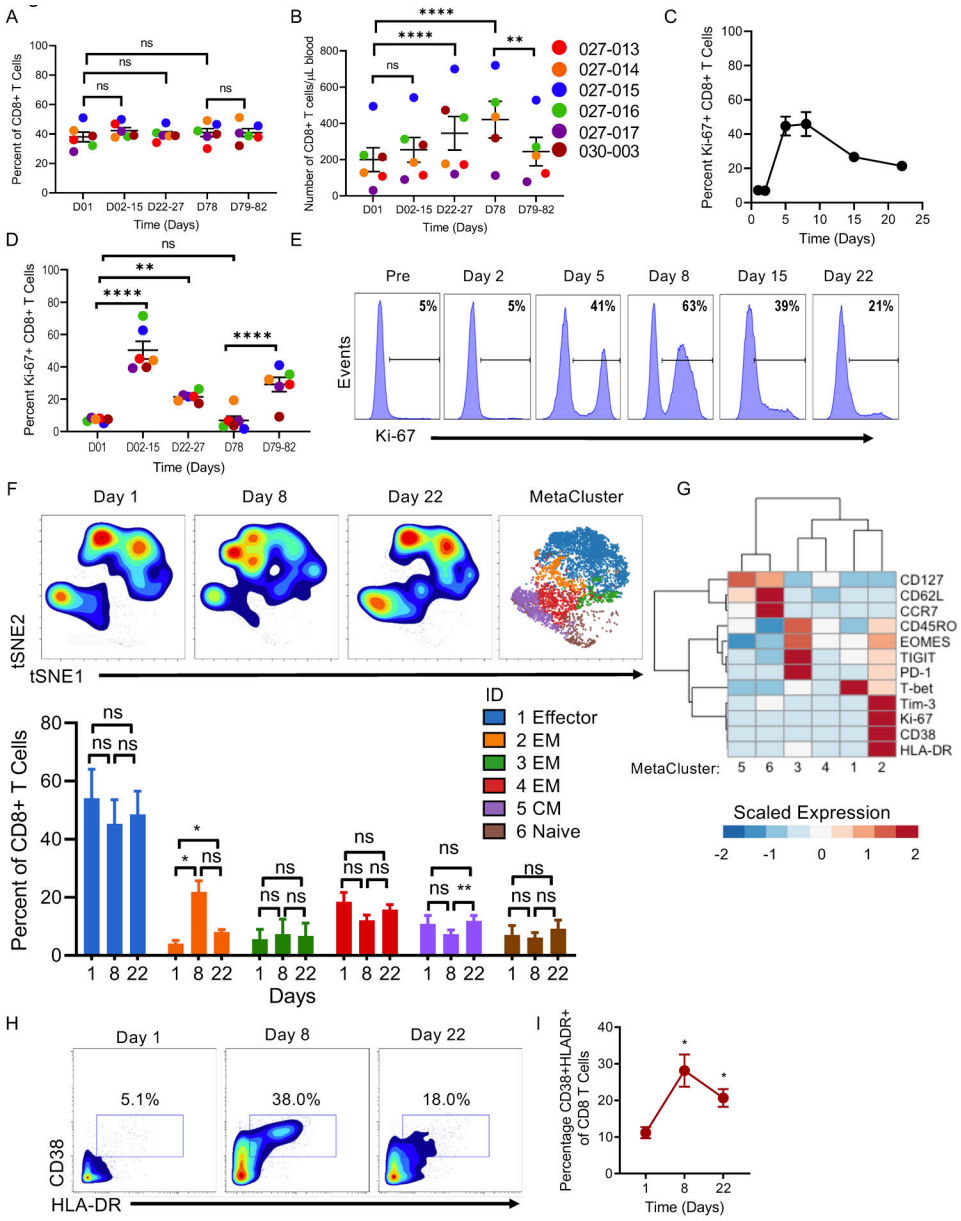

Figure 3. N-803 and rituximab expand and activate a subset of CD8+ T cells.

A) Dot Plot of the percent and B) absolute number of CD8 + T cells. C) Line graph and D) dot plots of percent of Ki-67+ CD8+ T cells by time point. Linear mixed model for all. E) Representative flow histograms of Ki-67 expression in CD8+ T cells at each time point. Numbers denote percent of Ki-67+ CD8+ T cells. F) *t*SNE density plot gated on CD8+ T cells and visualization of metaclusters from mass cytometry as determined by FlowSOM analysis, and bar graph of percent of each metacluster at each time point. 2-way ANOVA with Tukey's multiple comparisons. G) Relative expression of select CD8+ T cell markers in each metacluster. Expression is scaled by row. Friedman's test with Dunn's multiple comparisons. H) Representative plots of CD38 and HLA-DR expression in CD8+ T cells across time and I) percent of CD38 and HLA-DR double-positive T cells. RM one-way ANOVA with Dunnett's multiple comparisons test. Mean ± SEM for all line and dot plots.

Line graphs depict Mean ± SEM of values for all patients. n = 5-6, ≥ 3 independent experiments. Significance for mass cytometry comparisons $p < 0.05$, all others $p < 0.01$. * = $p < 0.05$, ** = $p \leq 0.01$, *** = $p \leq 0.001$, **** = $p \leq 0.0001$.

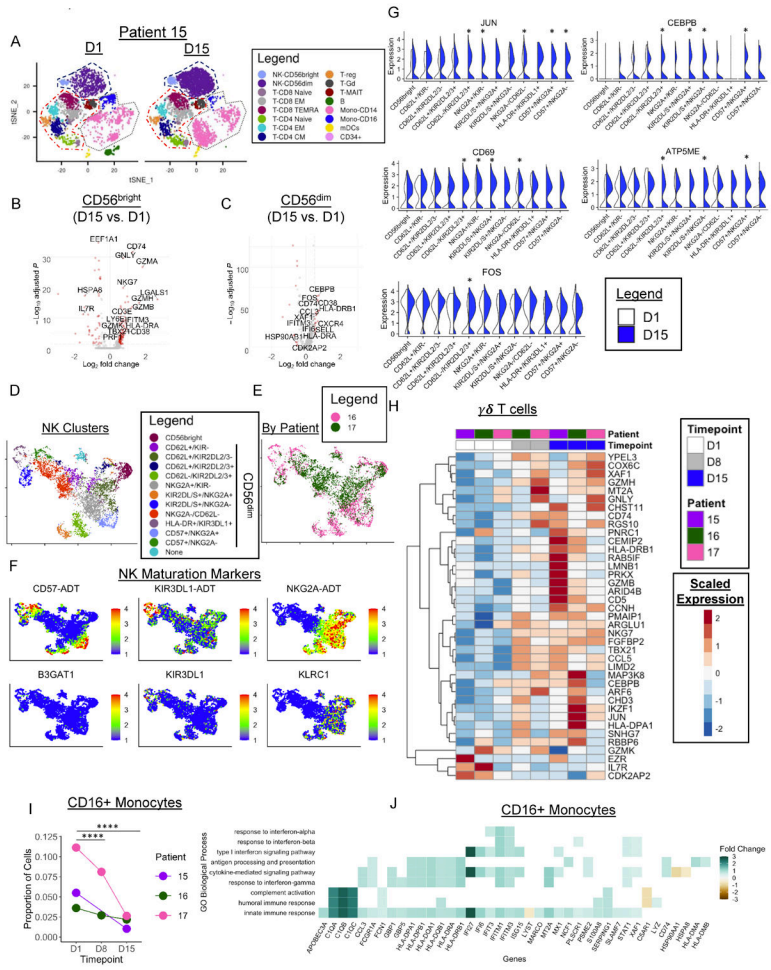

Figure 4. CITE-seq reveals activation of NK cells following N-803 plus rituximab.

A) *t*SNE visualization of PBMC transcriptomes colored by immune cell type in patient 027-015 (15) before (D1) and at D15 of N-803 plus rituximab. Dashed lines depict major immune cell lineages: NK (navy), T cells (red), Monocytes (grey). B-C) Volcano plots depicting summary data of the DEGs of all 3 patients in red in $CD56^{bright}$ and $CD56^{dim}$ NK cells with N-803 plus rituximab with an absolute $\log_2$ FC cut-off of ≥ 0.5. D) UMAP visualization of NK cell clusters in patients 027-016 (16) & 027-017 (17) clustered using CiteFuse with protein and RNA data. E) UMAP colored by patient. F) Feature Plots depicting protein (ADT) and RNA expression of key NK maturation markers. Min. cutoff = quantile 2 (q02), Max.cutoff = q98. G) Split violin plots depicting expression of select genes differentially expressed between D1 and D15 in each NK cell cluster. * denotes a significant change. White= Day 1, Blue = Day 15. H) Heatmap depicting select differentially expressed genes in $\gamma\delta$ T cells between pre-treatment (D1) and Day 15. I) Line graphs depicting the proportion of CD16 Monocytes in each patient at each timepoint. Two-sided fisher's Exact test with Holm's multiple comparisons p-value adjustment. * = $p < 0.05$, ** = $p \leq 0.01$, *** = $p \leq 0.001$, **** = $p \leq 0.0001$. J) Select enriched GO BP in CD16+ Monocytes between D15 and D1. Colored boxes depict average $\log_2$ FC of the genes in the BP gene set. White boxes correspond to genes not included in the GO BP gene set. Wilcoxon Rank-Sum test for

all DEGs with an adjusted p-value of < 0.05 and fold change of ≥ 0.5 absolute $\log_2$ fold change. Enriched GO terms $p < 0.05$ and q-value threshold of 0.05. n=2-3 patients for all. 2 independent experiments.

Table 1.

Patient demographics and baseline characteristics.

	No. of Patients	IV	SQ
Total number of patients treated	21	9	12
Sex			
Male	10 (48)	5 (56)	5 (42)
Female	11 (52)	4 (44)	7 (58)
Age years	63 (53-80)	62 (57-79)	64 (53-80)
iNHL Diagnosis			
FL	16 (76)	6 (67)	10 (83)
MZL	4 (19)	2 (22)	2 (17)
SLL	1 (5))	1 (11)	0 (0)
FLIPI risk (FL patients)	N=16	N=6	N=10
low	1 (6)	0 (0)	1 (10)
Int	8 (50)	2 (33)	6 (60)
High	7 (44)	4 (67)	3 (30)
Ann Arbor stage			
I	1 (5)	0 (0)	1 (8)
II	3 (14)	2 (22)	1 (8)
II	7 (33)	3 (33)	4 (33)
IV	10 (48)	4 (44)	6 (50)
Time since last treatment to N803	25 (1-134)	20 (1-88)	38 (1-134)
Median (range),months			
Time since last anti-CD20 to N803	27 (1-134)	22 (2-88)	52 (2-134)
Median (range), months			
Anti-CD20 status			
Sensitive	16 (76)	7 (78)	9 (75)
Refractory	5 (24)	2 (22)	3 (25)
Number of prior treatments	2 (1-7)	2 (1-7)	2 (1-7)
Median (range), n			
Prior Therapies			
Chemotherapy combination	17 (81)	8 (89)	9 (75)
Anti-CD20 monotherapy	4 (19)	1 (11)	3 (25)
Lenalidomide	1 (5)	1 (11)	0 (0)
PI3K inhibitor	2 (10)	1 (11)	1 (8)
BTK inhibitor	2 (10)	2 (22)	0 (0)
Radioimmunoconjugate	1 (5)	0 (0)	1 (8)
Auto SCT	1 (5)	1 (11)	0 (0)
Number of prior anti-CD20 treatments Median (range), n	2 (1-4)		

Table 2.

Adverse Events across both IV and SQ cohorts and all dose levels occurring in ≥10% of patients.

Adverse Event	IV or SQ (n=21)	IV (n=9)		SQ (n=12)	
	Gr1-3	Gr1-2	Gr3	Gr1-2	Gr3
Chills	19 (90)	7 (78)	-	12 (100)	-
Pyrexia	15 (71)	6 (67)	-	8 (67)	1 (8)
Fatigue	14 (67)	6 (67)	-	8 (67)	-
Injection site reaction	12 (57)	-	-	12 (100)	-
Nausea	11 (52)	6 (67)	1 (11)	4 (33)	-
Cough	9 (43)	4 (44)	-	5 (42)	-
Headache	8 (38)	3 (33)	-	5 (42)	-
Vomiting	8 (38)	5 (56)	1 (11)	2 (17)	-
Constipation	7 (33)	2 (22)	-	5 (42)	-
Pain	7 (33)	4 (44)	-	3 (25)	-
Diarrhea	6 (29)	1 (11)	-	5 (42)	-
Back pain	6 (29)	3 (33)	-	3 (25)	-
Hypotension	6 (29)	5 (56)	-	1 (8)	-
Alanine aminotransferase increased	5 (24)	3 (33)	-	2 (17)	-
Night sweats	5 (24)	1 (11)	-	4 (33)	-
Abdominal pain	4 (19)	4 (44)	-	-	-
Sinusitis	4 (19)	3 (33)	-	1 (8)	-
Lymphocyte count decreased	4 (19)	1 (11)	2 (22)	-	1 (8)
Myalgia	4 (19)	2 (22)	-	2 (17)	-
Dizziness	4 (19)	-	-	4 (33)	-
Dyspnea	4 (19)	3 (33)	-	1 (8)	-
Pruritus	4 (19)	3 (33)	-	1 (8)	-
Hypertension	4 (19)	-	2 (22)	-	2 (17)
Decreased appetite	2 (10)	-	-	2 (17)	-
Localized edema	3 (14)	-	-	3 (25)	-
Malaise	3 (14)	2 (22)	-	1 (8)	-
Edema peripheral	3 (14)	2 (22)	-	1 (8)	-
Aspartate aminotransferase increased	3 (14)	2 (22)	-	1 (8)	-
Blood alkaline phosphatase increased	3 (14)	1 (11)	-	2 (17)	-
Wheezing	3 (14)	2 (22)	-	1 (8)	-
Hyperglycemia	3 (14)	1 (11)	1 (11)	-	1 (8)
Anemia	2 (10)	1 (11)	1 (11)	-	-
Stomatitis	2 (10)	-	-	2 (17)	-
Influenza like illness	2 (10)	-	-	2 (17)	-
Peripheral swelling	2 (10)	1 (11)	-	1 (8)	-

Adverse Event	IV or SQ (n=21)	IV (n=9)		SQ (n=12)	
	Gr1-3	Gr1-2	Gr3	Gr1-2	Gr3
Skin infection	2 (10)	-	-	2 (17)	-
Upper respiratory tract infection	2 (10)	1 (11)	-	1 (8)	-
Urinary tract infection	2 (10)	-	--	2 (17)	-
Viral upper respiratory infection	2 (10)	1 (11)		1 (8)	-
Infusion related reaction	2 (10)	1 (11)	-	1 (8)	-
White blood cell count decreased	2 (10)	1 (11)	-	1 (8)	-
Hyponatremia	2 (10)	-	-	2 (17)	-
Dysgeusia	2 (10)	1 (11)	-	1 (8)	-
Peripheral sensory neuropathy	2 (10)	-	-	2 (17)	-
Presyncope	2 (10)	2 (22)	-	-	-
Somnolence	2 (10)	1 (11)	-	1 (8)	-
Dysuria	2 (10)	1 (11)	-	1 (8)	-
Actinic keratosis	2 (10)	-	-	2 (17)	-
Hyperhidrosis	2 (10)	1 (11)	-	1 (8)	-
Flushing	2 (10)	1 (11)		1 (8)	-